Probing Proton Damage in SOI CMOS Technology By Using Lateral Bipolar Action

Ying Li[1], Guofu Niu[1], John D. Cressler[2], Jagdish Patel[3], Mike Liu[4], Mohammad M. Mojarradi[3], Robert A. Reed[5], Paul W. Marshall[6], and Benjamin J. Blalock[7]

[1]Alabama Microelectronics Science and Technology Center, Electrical and Computer Engineering Department, 200 Broun Hall, Auburn University, Auburn, AL 36849, USA.
[2]School of Electrical and Computer Engineering, Georgia Institute of Technology, Atlanta, GA 30332, USA.
[3]Jet Propulsion Laboratory, Pasadena, CA 91109, USA.
[4]Honeywell Solid State Electronics Center, Plymouth, MN 55441, USA.
[5]NASA-GSFC, Code 562, Greenbelt , MD 20771, USA.
[6]Consultant to NASA-GSFC, Code 562, Greenbelt, MD 20771, USA.
[7]Department of Electrical and Computer Engineering, University of Tennessee, Knoxville, Tennessee 37966, USA.

35-Word Abstract

We investigate proton damage in SOI CMOS using lateral bipolar operational modes. The impact of interface states and oxide charge can be more clearly observed using lateral bipolar action than by using FET operational characteristics.

Author Contact Information:

Ying Li
200 Broun Hall, Electrical and Computer Engineering Department, Auburn University, Auburn, AL, 36849, USA
Tel: (334) 844-1865 / Fax: (334) 844-1888 / E-mail: yingli@eng.auburn.edu.

Suggested Session:
SOI and SOS Technologies
Radiation Effects on Electronic and Photonic Devices and Circuits

Student Paper
Oral Presentation Preferred

Probing Proton Damage in SOI CMOS Technology By Using Lateral Bipolar Action

Ying Li, Guofu Niu, John D. Cressler, Jagdish Patel, Mike Liu,
Mohammad M. Mojarradi, Robert A. Reed, Paul W. Marshall, and Benjamin J. Blalock

Abstract— **We investigate proton damage in SOI CMOS devices on UNIBOND using variety of lateral bipolar operational modes. We show that the impact of interface states and oxide charge can be more clearly observed using lateral bipolar action than by using normal FET operational characteristics. We also investigate the radiation-induced interface states at the Si/buried oxide interface and oxide charges in the buried oxide of a SOI CMOS technology using the DCIV method.**

I. Introduction

It is well known that proton radiation produces both displacement and ionization damage in semiconductor devices. In MOSFET characterization, the subthreshold $I_D - V_{GS}$ characteristics is widely used to identify the types of interface traps introduced by irradiation, as well as the resulting radiation-induced fixed oxide trapped charges. The change of $I_D - V_{GS}$, however, is often very small, making the identification of radiation-induced charges difficult, primarily because of the thin gate oxide found in modern devices. On the other hand, radiation-induced interface traps also act as recombination centers when an MOSFET is operated as a lateral bipolar transistor or a gated diode (body to source/drain). Electrical properties of the interface traps, including their energy levels and density, can be derived from the gate bias dependence of the recombination current [1] [2] [3], an analysis technique which can be dated back to the early 1960s [4].

We propose in this paper a new technique of identifying radiation-induced charge by using the collector current characteristics of a lateral bipolar transistor, and demonstrate its utility by applying it to the analysis of proton radiation damage in SOI CMOS devices on UNIBOND. This technique, together with conventional $I_D - V_{GS}$ measurements and $DCIV$ measurements [6], provides an effective toolset for radiation damage probing of advanced transistor technologies. We also investigate the radiation-induced interface states and oxide trapped charge for the back-gate transistor in SOI CMOS technologies using the DCIV method. The back-gate $DCIV$ spectra (I_B versus back-gate V_{GB} curves) clearly shows the radiation-induced changes in interface states at the Si/buried oxide interface, as well as fixed oxide charges trapped in buried oxide during irradiation, and hence is very useful for diagnostics on irradiated devices.

II. Experiment

The devices were fabricated using Honeywell's 0.35 μm partially-depleted SOI technology [5]. The SOI substrate here was formed by UNIBOND. The wafers were diced and attached to a ceramic holder and directly exposed to 62.5 MeV protons to equivalent gamma doses as high at 3 Mrad(Si) at the Crocker Nuclear Laboratory Cyclotron located at the University of California at Davis. The schematic diagram of our SOI MOSFETs is shown in Fig. 1. The body ties of the device cannot be seen in this two-dimensional figure because they are at the two ends of the front-gate.

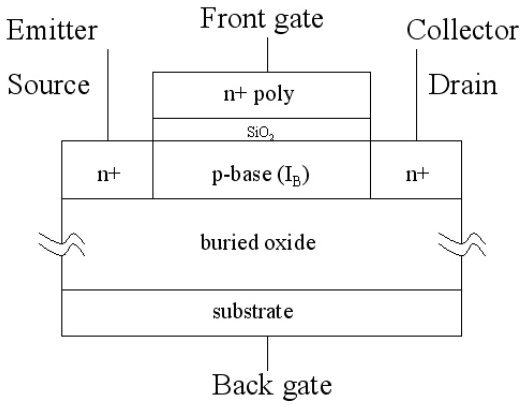

Fig. 1. The cross-section view of a basic SOI MOSFET structure.

III. Measurement Technique

In our measurements, the front-gate controlled I_B of the n^+ source (emitter) / p^- body (base) / n^+ drain (collector) lateral BJT for the nFET, and p^+ source (emitter) / n^- body (base) / p^+ drain (collector) lateral BJT for the pFET (V_{SB}=$V_{DB} = -V_{BE}$), were used to probe the recombination current from the interface traps which are distributed over the front-gate channel region. We also define a back-gate controlled mode by sweeping the back-gate voltage to obtain the base current I_B. Because the drain/source junctions go though the entire silicon film in this technology, under this back-gate controlled mode measurement, the base current can be also used to measure the recombination current from the interface traps generated during irradiation (or even fabrication) in the back-gate channel region.

This work was supported by the JPL CISM program under contract #1219281, DTRA under the Radiation Tolerant Microelectronics Program, NASA-GSFC under the Electronics Radiation Characterization (ERC) Program, and the Auburn University CSPAE under NASA contract # NCC5-549. The samples were fabricated at the Honeywell Solid State Electronics Center.

Y. Li and G. Niu are with the Alabama Microelectronics Science and Technology Center, Electrical and Computer Engineering Department, 200 Broun Hall, Auburn University, Auburn, AL 36849, USA. Tel: (334) 844-1865 / Fax: (334) 844-1888 / E-mail: yingli@eng.auburn.edu.

J. D. Cressler is with the School of Electrical and Computer Engineering, Georgia Institute of Technology, Atlanta, GA 30332, USA.

J. Patel and M.M. Mojarradi are with Jet Propulsion Laboratory, Pasadena, CA 91109, USA.

M. Liu is with Honeywell Solid State Electronics Center, Plymouth, MN 55441, USA.

R. A. Reed is with NASA-GSFC, Code 562, Greenbelt, MD 20771, USA.

P. W. Marshall is a consultant to NASA-GSFC, Code 562, Greenbelt, MD 20771, USA.

B. J. Blalock is with Department of Electrical and Computer Engineering, University of Tennessee, Knoxville, Tennessee 37966, USA.

IV. Results and Discussion

A. Front-Gate Transistor

Consider an SOI MOSFET exposed to 1.3 Mrad and 3 Mrad radiation levels. The pre- and post-radiation front-gate $I_D - V_{GS}$ characteristics are shown in Fig. 2 for a 10/0.35 (W/L=10μm/0.35μm) nFET. A close inspection shows that the threshold voltage first increases with increasing dose, and then decreases with further dose. This can be attributed to the combined effects of interface traps (which increases V_{th}) and oxide trapped charge (which decreases V_{th}) [5]. The shift of the subthreshold $I_D - V_{GS}$ characteristics, however, is quite small, because of the thin front gate oxide (8 nm in this case). Furthermore, it is impossible to make any meaningful identification of the shift in I_D for lower front gate voltages, since I_D is below the measurement limit. This is unfortunate, since the shift here gives useful information on the interface trap density for traps near the middle of the bandgap.

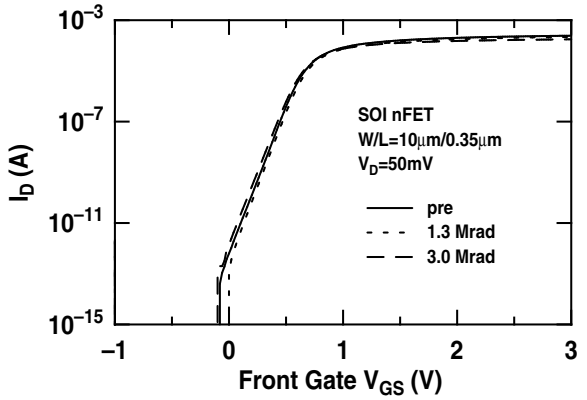

Fig. 2. Front-gate subthreshold characteristics of a 10μm / 0.35 μm SOI nFET.

Recall that the subthreshold drain current can also be viewed as the collector current of the underlying lateral bipolar transistor. The essential difference between this device and a standard BJT is that the base bias is provided through the gate oxide capacitance. We can therefore increase the drain current by simply forward-biasing the source-body junction, which provides a much stronger bipolar action. To better examine the properties of the radiation-induced interface charges as a function of gate voltage, we measure the collector current I_C (or the drain current) as a function of base-emitter voltage V_{BE} (or body-source voltage) using the gate-body voltage (V_{GB}) as a variable. Typical results are shown in Fig. 3 for the same device shown in Fig. 2. The collector is grounded and thus V_{CB}=0V. The $I_C - V_{BE}$ characteristics is typical of a bipolar transistor except at high V_{GB} and high V_{BE}, when the surface is inverted. The benefits of such a bipolar operation measurement include: 1) the net charge at the interface is more easily identified for each gate voltage. 2) The interface trap information at lower V_{GB} (and hence near the middle of the bandgap) can be obtained, due to the higher I_C enabled by the explicit forward V_{BE}.

In Fig. 3, at V_{GB}=-0.5V, one can clearly identify a decrease of I_C at 1.3 Mrad, and a subsequent increase of I_C as the radiation dose increases to 3 Mrad. This observation is consistent with what one would expect by extrapolating the subthreshold $I_D -$

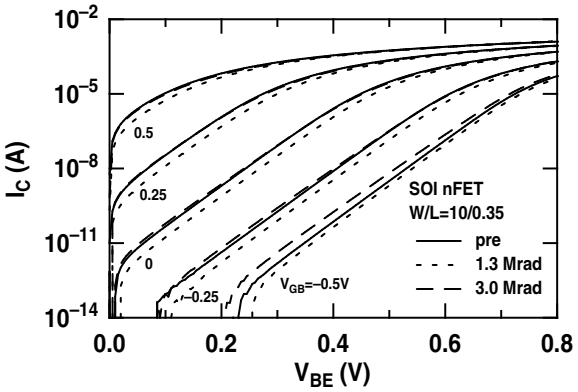

Fig. 3. The collect current versus the base-emitter current for a 10μm / 0.35 μm SOI nFET at the different gate-base voltages.

V_{GS} curve to the lower V_{GS} range. However, the identification from Fig. 3 is direct, and much easier in practice. At V_{GB}=0V, the I_C at 1.3 Mrad is obviously lower than at pre-radiation, and the I_C at 3 Mrad is about the same as at pre-radiation.

The front-gate controlled I_B curves with a V_{BE} of 0.3V are given in Fig. 4 for the same device shown in Fig. 3. The radiation-generated increase of I_B gives a direct measure of the surface recombination velocity S_0 and the density of the interface traps, N_{IT}, because they are proportional to the maximum of the radiation-induced ΔI_B [6]. Here, $\Delta I_B = I_B$-I_{BL}, where I_{BL} is the V_{GB} independent baseline. The baseline current I_{BL} physically comes from electron-hole recombination in the bulk and surface traps located outside the p-channel, and hence are not modulated by the gate voltage V_{GB} [7] when the channel is in accumulation. However, in Fig. 4, the increase of base current with radiation dose in the accumulation region can be clearly observed and is attributed to majority carrier tunneling at the p/n junction perimeter under the gate oxide. With increasing radiation dose, this majority carrier tunneling process increases because the radiation-induced displacement damage increases defects at the corner of gate and drain (source) regions. A similar increase of I_B after radiation can also be observed for a 10/0.35 pFET.

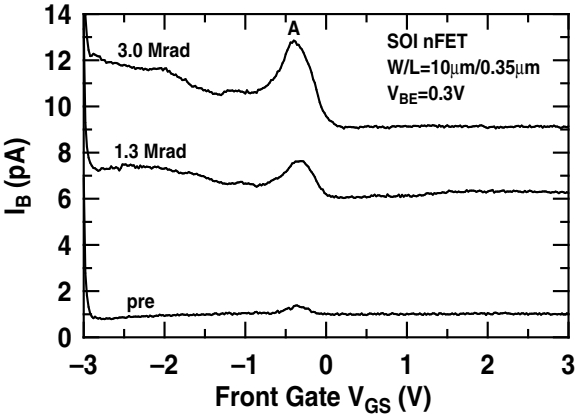

Fig. 4. The gate-controlled I_B curves for a 10μm / 0.35 μm nFET.

Fig. 5 shows the channel length normalized ΔI_B peak versus dose for 10/0.35, 10/0.5, 10/10 nFETs having the same chan-

nel width, but different channel lengths. It can be clearly seen that the value of the ΔI_B peak is channel-length dependent, because the radiation-induced interface traps are distributed along the front gate channel. We can also see that the ΔI_B peak increases linearly with radiation dose for each device and has not reached a saturation value up to 3 Mrad total dose, which means the N_{it} is not saturated at the front Si/oxide interface up to 3 Mrad. The shorter the devices are, the more sensitive they are to interface traps, and thus they experience a more rapid increase of ΔI_B than in the longer devices.

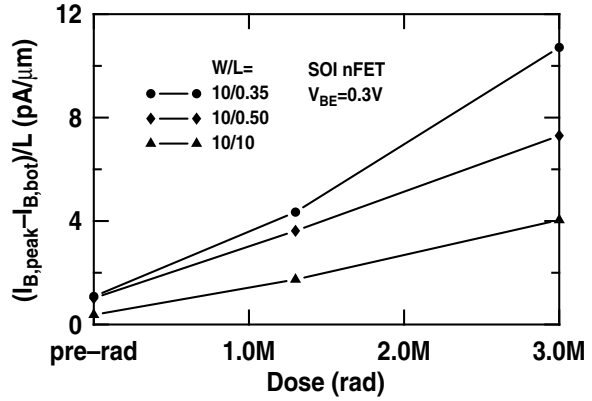

Fig. 5. Channel length normalized ΔI_B peak versus dose for a 10/0.35, 10/0.50 and 10/10 nFETs.

B. Back-Gate Transistor

The back-gate controlled I_B is measured when the front-gate channel is accumulated (front-gate $V_{GB} = -1V$ for the nFET and front-gate $V_{GB} = 1V$ for the pFET) to minimize recombination at the Si/front-gate oxide interface. The measured I_B is then primarily due to recombination at the Si/buried oxide interface or in the silicon film body. The back-gate controlled I_B for a 10/10 nFET is shown in Fig. 6 at V_{BE}=0.4V. Three peaks (peak A, peak B and peak C) can be clearly observed for both pre- and post-radiation. Note that I_B increases after radiation, which is attributed to the increase of the number of recombination centers due to radiation damage.

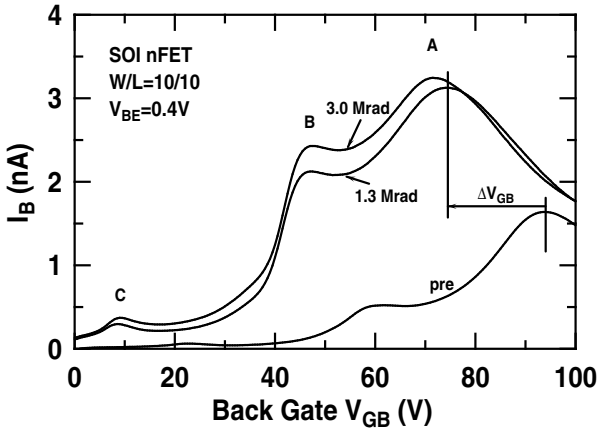

Fig. 6. Back-gate controlled I_B curves for a 10/10 nFET at V_{BE}=0.4V.

In the MOSFET $I_D - V_{GS}$ curves, a nearly parallel shift occurs after radiation, as shown in Fig. 7. Therefore, the dominant charge induced by radiation is oxide trapped charge. The interface charge, which is modulated by the gate voltage, plays a much smaller role. Unlike the MOSFET subthreshold $I_D - V_{GS}$ curves, the post-irradiation $DCIV$ spectra is not a simple shift of the pre-irradiation $DCIV$ spectra. However, the shifts of voltage position of the peaks are considerably different from the shift of the back gate $I_D - V_{GS}$ curve. At 1.3 Mrad, the shifts are 19.5 V for peak A, and 14 V for peaks B and C. The shift of the subthreshold $I_D - V_{GS}$ curve, however, is 16.8 V. Given the fact that the shift of the $I_D - V_{GS}$ curve is nearly independent of V_{GS}, we conclude that the energy level distribution of interface traps differs between pre- and post-irradiation. Without a change in the energy level distribution, the change of the $DCIV$ spectra would be similar to the change of the $I_D - V_{GS}$, except for an increase in the magnitude of I_B.

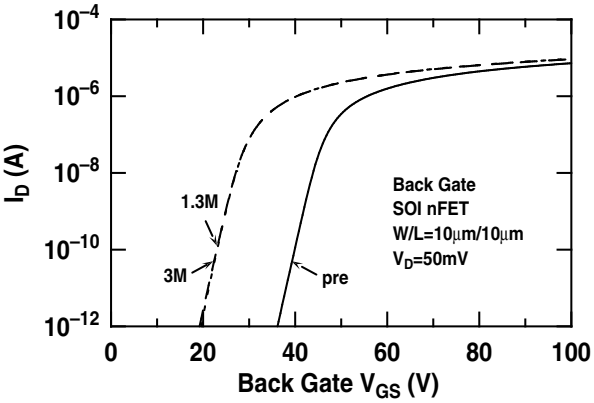

Fig. 7. Back-gate subthreshold characteristics of a 10/10 nFET before and after radiation.

Another logical question is whether the three peaks observed simply indicate that there are three dominant discrete trap energy levels. To answer this question, we plot $\Delta I_{B,peak}$ versus V_{BE} on semilog scales for each peak. The result for peak A is shown in Fig. 8. Theory for a discrete energy level interface trap predicts that $\Delta I_{B,peak} \propto \exp(qV_{BE}/nkT)$, with $n = 1$ when $V_{BE} \ll V_{BE-ET}$, $n = 2$ when $V_{BE} \gg V_{BE-ET}$, and the transition from $n = 1$ to $n = 2$ occurs within 100 mV. Here V_{BE-ET} is determined by the trap energy level as $2(E_T - E_I)/q + [\ln(c_{ns}/c_{ps} - 1.4]kT/q$, with E_T being the trap energy level, E_I being the intrinsic Fermi-level, and C_{ns} and C_{ps} being the electron and hole capture rate coefficients at this trap energy level [7]. The data measured, however, does not show this behavior for peak A, either at pre-radiation or post-radiation. Instead, the data can be fit using a single n factor *over a wide range of* V_{BE}. In this case, n = 1.82, 1.79, 1.75 for pre-radiation, at 1.3 Mrad and 3 Mrad doses, respectively. This dependence strongly suggests that the distribution of the interface states (both pre- and post-radiation) is relatively flat, despite the three noticeable peaks on the $DCIV$ spectra. The shape of the distribution, as discussed above, is changed considerably after irradiation, because of different shifts for the different peaks. We also have determined that that the n factor is 1.6 for peak B and 2.0 for peak C.

Different back-gate controlled I_B curves can be observed in Fig. 9 for a 10/10 pFET, both before and after irradiation. There are only two observable peaks (noted as peak A and peak B) and

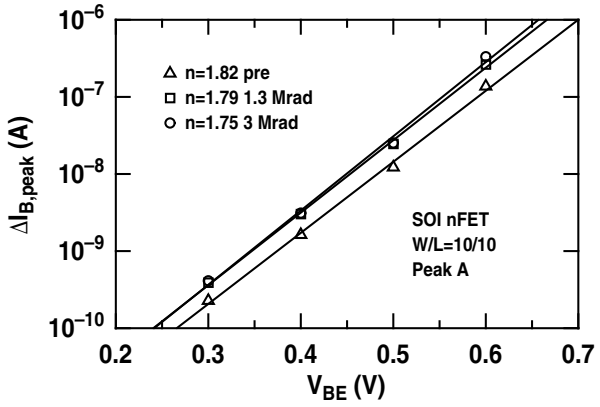

Fig. 8. Variation of $\Delta I_{B,peak}$ with the forward bias V_{BE} from pre and after two radiation doses. The lines are exponentially fit to the experimental data.

peak A is much sharper than any peaks observed in the back-gate $DCIV$ spectra of the nFETs as shown in Fig. 6. This suggests a more concentrated interface state distribution (in the bandgap) than for the nFET. At 1.3 Mrad, the $I_D - V_{GS}$ shift is -10.3 V. The shifts in peak A and B, however, are -15.5 and -10.0 V. This clearly indicates that the energy distribution of the interface traps has changed after irradiation, for reasons similar to the nFET case. It is also clearly shown that $I_{B,peak}$ of peak B equals to that of peak A before radiation. However, with increasing radiation dose, the $I_{B,peak}$ of peak A increases quickly and exceeds that of peak B at 1.3 Mrad radiation. This suggests that radiation-induced interface traps are concentrated at the same energy level as that for peak A. Similar I_B versus back-gate V_{GB} characteristics can also be observed for the 10/0.35 pFET.

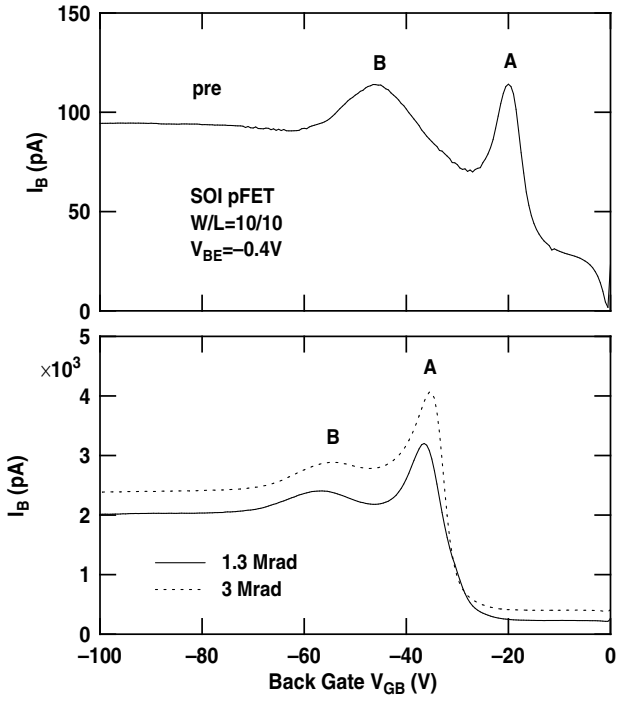

Fig. 9. Back-gate $DCIV$ spectra for a 10/10 pFET: 1) pre-radiation, 2) after 1.3 Mrad, and 3) after 3 Mrad.

Even though the nFETs and pFETs share the same back-gate oxide, they show a different back-gate radiation response, as can be seen in Fig. 10 for the 10/10 nFET and pFET. It is clearly seen that the recombination current of the pFET back-gate channel is much smaller than that in nFET back-gate channel for pre-irradiation. Below 1.3 Mrad radiation, the I_B peak for the pFET increases more quickly than for the nFET, while above 1.3 Mrad, the recombination current of the pFET is almost as same as that of the nFET. For the nFET, on the other hand, the recombination current saturates after 1.3 Mrad. Note, however, that the recombination current of the pFET still increases though at a much slower rate than below 1.3 Mrad.

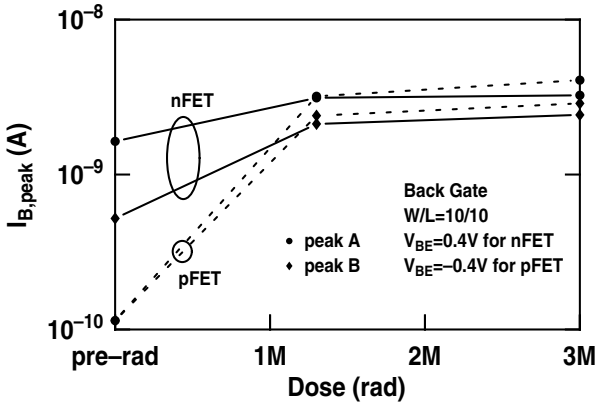

Fig. 10. Back-gate controlled I_B peak versus dose for a 10/10 nFET and a 10/10 pFET.

V. Summary

We have investigated radiation damage in SOI CMOS on UNIBOND devices using a new technique which identifies radiation-induced charge using the collector current in bipolar operational mode, and have applied it to studying proton damage in these devices. This technique, together with conventional $I_D - V_{GS}$ measurements and $DCIV$ measurements, provides an effective toolset for radiation damage probing of modern SOI technologies. Using $DCIV$, the energy distribution of radiation-induced interface states is investigated for the back-gate transistor in this SOI CMOS technology. We find that the energy distribution of the interface states is significantly changed by proton irradiation. Different back-gate radiation behavior between nFETs and pFETs are clearly observed in the back-gate $DCIV$ spectra, suggesting a different damage mechanism between the two devices.

Acknowledgment

The devices were fabricated at Honeywell. The authors would like to thank L. Cohn, K. LaBel, and H. Brandhorst for their support of this work.

References

[1] G. Niu *et al.*, *IEEE Trans. Nuclear Science*, vol. 45, p. 2361, Dec. 1998.
[2] M.-S Park *et al.*, *IEEE Trans. Nuclear Science*, vol. 48, p. 2285, Dec. 2001.
[3] D.R. Ball *et al.*, *IEEE Trans. Nuclear Science*, vol. 49, p. 3185, Dec. 2002.
[4] C.T. Sah, *Proc. of IRE*, vol. 49, p. 1623, Nov. 1961.
[5] Y. Li *et al.*, *IEEE Trans. Nuclear Science*, vol. 49, p. 2930, Dec. 2002.
[6] A. Neugroschel *et al.*, *IEEE Trans. Electron Devices*, vol. 42, p. 1657, Sept. 1995.
[7] J. Cai *et al.*, *IEEE Electron Device Letters*, vol. 20, p. 60, Jan. 1999.